Published in final edited form as:

Neuroscience. 2017 February 20; 343: 240–249. doi:10.1016/j.neuroscience.2016.11.046.

Axial levodopa-induced dyskinesias and neuronal activity in the dorsal striatum

Stephanie L. Alberico[1], **Young-Cho Kim**[1], **Tomas Lence**[1], and **Nandakumar S. Narayanan**[1]

[1]Department of Neurology, Carver College of Medicine, University of Iowa, Iowa City, IA 52242, 4 United States

Abstract

Levodopa-induced dyskinesias are abnormal involuntary movements that limit the effectiveness of treatments for Parkinson's disease. Although dyskinesias involve the striatum, it is unclear how striatal neurons are involved in dyskinetic movements. Here we record from striatal neurons in mice during levodopa-induced axial dyskinesias. We developed an automated 3-dimensional motion tracking system to capture the development of axial dyskinesias at ~10 ms resolution, and correlated these movements with neuronal activity of striatal medium spiny neurons and fast spiking interneurons. The average firing rate of medium spiny neurons increased as axial dyskinesias developed, and both medium spiny neurons and fast spiking interneurons were modulated around axial dyskinesias. We also found that delta field potential power increased in the striatum with dyskinesia, and that this increased delta power coupled with striatal neurons. Our findings provide insight into how striatal networks change as levodopa-induced dyskinesias develop, and suggest that increased medium spiny neuron firing, increased delta field potential power, and abnormal delta-coupling may be neurophysiological signatures of dyskinesias. These data could be helpful in understanding the role of the striatum in the pathogenesis of dyskinesias in Parkinson's disease.

Keywords

Levodopa-induced dyskinesia; tracking; Parkinson's disease; fast spiking interneurons; medium spiny neurons

INTRODUCTION

Motor symptoms of Parkinson's disease (PD) are most often treated using L-3,4-dihydroxyphenylalanine (L-DOPA or levodopa), a dopamine precursor. However, 80% of PD patients develop levodopa-induced dyskinesias (LIDs), which are abnormal, involuntary movements (Ahlskog and Muenter, 2001). LIDs are a major challenge in treating PD

Corresponding Author. Nandakumar Narayanan, 319-353-5698, Nandakumar-narayanan@uiowa.edu, 169 Newton Road, Pappajohn Biomedical Discovery Building – 1336, University of Iowa, Iowa City, 52242.

because they limit the usefulness of levodopa, the most effective and commonly used therapy. In addition, the development of LIDs are harbingers of more invasive and high-risk PD therapies such as deep-brain stimulation (Fahn et al., 2004).

The mechanism by which LIDs develop remains unknown. PD involves degeneration of midbrain dopaminergic neurons which heavily project to the striatum (Alberico et al., 2015). Rodent and primate PD models also develop LIDs with chronic levodopa exposure; even in animals with dopamine depletion restricted to the dorsal striatum (Lundblad et al., 2004, 2005; Pavón et al., 2006; Santini et al., 2007). The dorsal striatum is largely comprised of medium spiny neurons (MSNs), which are the primary output neuron of the striatum. Most MSNs express dopamine receptors (Gerfen, 2000; Kreitzer, 2009). Dopamine increases excitability in MSNs expressing D1-type dopamine receptors, promoting movement, and decreases excitability in MSNs expressing D2-type dopamine receptors (Surmeier et al., 2007; Cui et al., 2013). PD involves a progressive loss of dopaminergic input to the striatum, disrupting both D1 and D2 MSNs leading to the motor symptoms of PD (Bunney et al., 1973; Hernandez et al., 2013). Although comparatively rare, fast spiking interneurons (FSIs) are positioned to powerfully influence MSNs and in turn affect movement (Berke, 2011). FSIs can powerfully modulate the firing of MSNs (Koós and Tepper, 1999; Planert et al., 2010). FSIs also have dopamine receptors and provide strong feedforward inhibition of MSN activity, and thus may play a role in dyskinesias (Bracci et al., 2002; Centonze et al., 2003; Koos et al., 2004; Gittis et al., 2011b). Dopamine depletion can have complex effects on MSNs and FSIs as a result of altered input to striatum and/or remodeling of intrastriatal networks (Prosperetti et al., 2013; Corbit et al., 2016; Kondabolu et al., 2016). These may contribute to dysfunctional striatal networks and the emergence of synchrony at beta frequencies (Mallet et al., 2006; Jenkinson and Brown, 2011).

Here, we examine the neuronal activity of dorsal striatal neurons in LIDs. We record from MSNs, FSIs, and striatal local field potentials (LFPs) as dopamine-depleted mice develop LIDs. Striatal LFPs are of particular translational significance because they can be directly measured in humans via intracranial recordings. While these LFPs have been implicated in PD it is unknown how they change as LIDs develop (Brown et al., 2001; Williams et al., 2002; Brown and Williams, 2005). A significant challenge to resolving these issues is that prior studies have human raters score abnormal involuntary movements as a measure of LIDs in rodents (Lundblad et al., 2002; Winkler et al., 2002; Smith et al., 2011; Breger et al., 2013). In this method, humans grade axial, limb, and orofacial dyskinesias over a 1–2 minute window every several minutes (Lundblad et al., 2005; Cenci and Lundblad, 2007; Santini et al., 2007). This technique is not suited to capture modulation of striatal MSNs, which can be correlated with movements on the scale of milliseconds (Lundblad et al., 2004; Cenci and Lundblad, 2007; Breger et al., 2013; Sgroi et al., 2014). To address these issues, we used 3-dimensional position tracking technology to capture animals' position at ~10 ms and ~ 1 mm resolution while recording neuronal activity from the dorsal striatum of mice during the development of LIDs. We found that striatal FSIs and MSNs changed firing with dyskinesias and were modulated around axial LIDs. These observations provide novel insight into the role of striatal neurons in LIDs.

EXPERIMENTAL PROCEDURES

Animals

We used 9 C57/BL6 male mice (Harlan, Madison, WI), weighing >25g at the time of dopamine depletion. All procedures were approved by the Animal Care and Use Committee at the University of Iowa.

LID induction

We induced dyskinesias as previously described (Figure 1A; Lundblad et al., 2004; Cenci and Lundblad, 2007). Briefly, mice were anesthetized using ketamine (100 mg/kg) and xylazine (10 mg/kg) and injected with desipramine (25 mg/kg; i.p.) to protect catecholaminergic neurons. First, we depleted dopamine in the medial forebrain bundle (MFB) using the neurotoxin 6-OHDA bromide (Sigma, St. Louis, MO) made each surgery day at a concentration of 1 μg/μL dissolved in 0.02% ascorbic acid (AVANTOR, Central Valley, PA). Animals were unilaterally depleted of dopamine with 1μg of 6-OHDA stereotaxically injected into the MFB (AP: −1.2, ML: −1.2, DV: −4.7 from dura). We found that 1 μg of 6-OHDA reliably caused 71±5% (mean±SEM) dopamine depletion in the striatum. With levodopa administration this dopamine-depletion protocol maximized LIDs and minimized mortality of mice with electrode implants (Figure 1B). In these animals, a 16 channel stainless steel microwire array (50 μm, 4×4; MicroProbes, Gaithersburg, MD) was lowered into the dorsal striatum (AP: +0.1, ML: −2.0, DV: −3.0; Figure 1B) while measuring neuronal activity. To ground the electrode, the stainless steel ground wire was wrapped around two skull screws, which were placed over the contralateral lateral surface of the skull between the bregmatic and lambdoid sutures. The craniotomy was sealed and implants were fixed in place with cyanoacrylate ('SloZap', Pacer Technologies, Rancho Cucamonga, CA) and methyl methacrylate (dental cement; AM Systems, Port Angeles, WA). In addition, an implant was designed to attach two 4 mm infrared reflective spheres to the recording headstage (Figure 2A). Following a week of recovery, animals were tested for unilateral depletion with the amphetamine-induced rotation test. Animals were injected with amphetamine (5 mg/kg; i.p.) and ipsilateral rotations were recorded 30 min post-injection (Healy-Stoffel et al., 2012; Chotibut et al., 2013). Animals that did not show >5 ipsilateral rotations per minute were not included in this study (Chang et al., 1999; Paquette et al., 2009); animals used in the study performed 11±2 ipsilateral rotations per minute. Only complete rotations (360°) were counted. On the day following amphetamine-induced rotation testing, we began administering 20 mg/kg of L-DOPA-methylester (levodopa; Sigma) dissolved in 0.09% NaCl sterile saline at a concentration of 4 mg/mL with Benserazide (2 mg/mL; Sigma) daily. Striatal neuronal activity was recorded on Day 1 and Day 13 of levodopa administration while tracking movements (Figure 2).

Abnormal involuntary movement scores

We used amplitude based scoring to characterize LIDs in our mouse model (Lundblad et al., 2002; Winkler et al., 2002; Smith et al., 2011; Breger et al., 2013). Briefly, animals were assessed for two minutes every 10 minutes for an hour and each LID subtype was given two scores, one for duration of dyskinesias (0–4) and one for severity (0–4). These scores were then multiplied and axial, orofacial, and limb LID subtypes were added to obtain the

integrated AIM scores at each time point (Figure 3A, line graph). To obtain a global score, integrated AIM scores were summed for each recording session (Figure 3A).

Automated computer tracking

For 13 days, animals were injected with 20 mg/kg of levodopa (Figure 1A). Starting on Day 1 with baseline recording before levodopa administration, striatal activity was recorded along with behavior via OptiTrack Prime 13 cameras (NaturalPoint Inc, Corvallis, OR) using Motive OptiTrack software and a video camera at the beginning and end of treatment (Day 1 and 13) to measure the development of LIDs. The OptiTrack cameras were mounted on tripods with a height of 34 cm from recording surface (Figure 2A). These cameras were calibrated on each recording day using a wand (250 mm; NaturalPoint Inc) consisting of three infrared reflective spheres at a fixed distance from one another in a straight line. The filter switch on Motive OptiTrack was set to infrared spectrum, the gain was set to “low” for short range, and the cameras were set to object mode. At least 5000 samples were gathered to calibrate the cameras. A sample is registered when two or more cameras can view all three spheres. Following wand calibration, the ground plane (X, Y, Z directions) was set by placing a calibration square (NaturalPoint Inc) with three infrared reflective spheres. Wand calibration was applied and converted to meters and the output had a mean 3-dimensional error of <.03 mm. Two 4-mm infrared reflective spheres were attached to the headstage to determine animals’ head position. The animals were placed in a transparent cylinder (15 cm diameter) 42 cm from each camera (Figure 2A). Motive OptiTrack was synced with Plexon and with the video camera. The Motive Optitrack software tracks movements along the X, Y, and Z axes. Position data were exported as CSV files using Motive OptiTrack. Basic tracking of two infra-red reflective spheres on the animal’s head was done in Motive. When Motive lost tracking of the spheres due to reflection from the recording chamber, coordinates of the spheres were co-registered in MATLAB using a nearest neighbor algorithm. The distance between the spheres in 3D space was calculated between n and n+1 frame, and minimal distance change per each detected sphere was selected as n+1 tracked sphere. Frames with no detected spheres were linearly interpolated when continuous missing frames were less than 1 second; otherwise these frames were excluded from behavioral analysis. A total of 96.9±0.8% frames were tracked per each session and linear interpolation filled in 2.8±0.7% of missing frames.

Rapid and continuous head rotation movements were identified as characteristic of axial dyskinesia-associated movements based on hand-scored dyskinesias. Head rotation was identified by simultaneous velocity changes in X and Y axes. Tracked sphere coordinates were filtered with a low-pass FIR filter at 4Hz to remove high frequency noise. Velocity was calculated between frames on the X and Y axes, then dyskinesia-associated head rotations were identified using *findpeaks* function in MATLAB. The threshold parameters for rotational movement were minimum peak prominence (continuous velocity changes) at 0.002 and minimum peak height (velocity) at 0.096 mm/sec.

Neuronal Analyses

Neuronal ensemble recordings in the striatum were made using a multi-electrode recording system (Plexon, Dallas, TX). Putative single neuronal units were identified on-line using an

oscilloscope and audio monitor. Plexon Off-line Sorter was used to analyze the signals after the experiments and to remove artifacts. Spike activity was analyzed for all cells that fired at rates above 0.1 Hz. Statistical summaries were based on all recorded neurons. Principal component analyses (PCA) and waveform shapes were used for spike sorting. Single units were identified as having 1) consistent waveform shape, 2) separable clusters in PCA space, and 3) a consistent refractory period of at least 1 ms in interspike interval histograms. All neurons were analyzed offline using Off Line Sorter (Plexon) and MSNs and FSIs were identified by waveform shape, half-peak-width, peak-to-trough duration, and firing rate (Figure 4A–B). Analysis of neuronal activity and quantitative analysis of basic firing properties were carried out using NeuroExplorer (Nex Technologies, Littleton, MA), and MATLAB. LFP channels were filtered between 0.7 and 1000 Hz online, sampled at 1000 Hz and recorded in parallel with single unit channels using a wide-band board. Medium spiny neurons and fast spiking interneurons were clustered using Gaussian mixture models.

Field potentials (4 per animal) were low-pass filtered at 0.5 Hz and high-pass filtered at 50 Hz using EEGlab's *eegfilt*. Spectrograms were calculated using EEGlab's *spectopo* using the entire recording session (Delorme and Makeig, 2004; Emmons et al., 2016). Power was compared via a paired-t test between sessions in three frequency bands: delta (1–4 Hz), theta (4–8 Hz), and beta (12–25 Hz). Spike-field coherence was calculated using neurospec's *sp2a_m1* using type 0 analysis, and a segment power of 11 with the average LFP per each animal according to methods described in detail previously (Rosenberg et al., 1989; Halliday et al., 1995, 1998; Parker et al., 2014). Coherence values were normalized to the 95% confidence interval for each neuron to facilitate comparisons across animals. All statistics assumed each recording day was an independent sample; no statistical dependence between days was considered and the same neurons were not explicitly tracked across days.

Histology

After the completion of the experiments, mice were euthanized by injections of 100 mg/kg sodium pentobarbital, and transcardially perfused with 4% paraformaldehyde. Brains were post fixed in 4% paraformaldehyde and cryoprotected in 30% sucrose before sectioning in a cryostat. Brain slices were mounted and stained for tyrosine hydroxylase (TH; polyclonal rabbit anti-TH, 1:500; Millipore, Temecula, CA) and cell bodies using DAPI. Histological reconstruction was completed using post mortem analysis of lesion, electrode placement in the striatum, and cell concentration in the substantia nigra. Images were captured on Zeiss Apotome.2 Axio Imager and cells in the substantia nigra were counted using the optical fractionator in Stereo Investigator for dopamine depletion quantification and analysis.

Statistics

All statistical testing was done via functions in the statistical toolbox in MATLAB. Hypotheses about levodopa administration affecting the development of LIDs, the firing rate of MSNs, FSIs, and LFPs were determined beforehand. Means of two independent populations were compared via a t-test. When a single group underwent repeated testing (i.e. comparing LIDs between Day 1 and 13), we used an ANOVA. We used a χ^2 test when counting elements (i.e. the number of neurons with spike-field coherence) in two

populations. In line with our past work, all neuronal populations were considered statistically independent over repeated days (Parker et al., 2014, 2015a, 2015b).

RESULTS

Automated tracking of LIDs

To induce LIDs, dopamine was unilaterally depleted using 1μg of 6-OHDA, after which levodopa (20 mg/kg) was administered for two weeks (Figure 1A). Mice were implanted with microwire recording arrays (16 channels, 4×4 array) into the dorsal striatum. Following one week of recovery, animals were screened for ipsilateral rotation using amphetamine. Only animals with biased and constant ipsilateral rotations were included in this study. On average, animals had a 71±5% decrease in TH positive cells in the substantia nigra pars compacta ($t_{(4)}$= 3.3, p<0.03; bar graph in Figure 1B). The average dopamine depletion we observed was lower than other studies (Lundblad et al., 2004, 2005; Cenci and Lundblad, 2007) due to the fact that we used 1μg of 6-OHDA, instead of 3μg. However, all mice developed LIDs and we observed minimal mortality. In these animals, we studied how striatal neuronal ensembles changed as LIDs developed on Day 1 vs. Day 13 of levodopa administration.

Along with microwire array implantation, all mice had two 4 mm infrared-reflective spheres attached to the recording headstage in the anterior-posterior dimension (Figure 2A). Four infrared cameras recorded the X (right and left), Y (forward-back), and Z (up-down) coordinates of the mouse's head at 120 frames/per second (frames/s) to track head position (Figure 2A). Automated computer tracking data was synchronized with a video camera at 30 frames/s and Plexon neurophysiological recording hardware (Figure 2B–C). To examine how movement tracking captured dyskinetic movements, we analyzed movement videos to identify dyskinetic movements by hand, and abnormal-involuntary movement (AIM) scoring was performed by human raters in LID sessions (Figure 3A; Winkler et al., 2002; Lundblad et al., 2004, 2005; Cenci and Lundblad, 2007; Bido et al., 2011; Smith et al., 2011). AIM scoring indicated that LIDs developed and increased severity over two weeks of levodopa administration in 6-OHDA-lesioned mice ($t_{(4)}$= 4.71, p< 0.01; Day 1 vs. Day 13) but not in sham-lesioned mice (Figure 3A). We recorded the timestamps of hand-coded LIDs along with tracking data (Figure 3B). By aligning automated tracking to video and hand-scoring, we found that axial LIDs involved large changes in the X and Y axes, with smaller changes in the Z axis (Figure 3B–C).

By examining patterns of movement in 3D around hand coded dyskinetic events, we observed that axial dyskinesias were associated with rapid changes in velocity and angular position, identified by peaks in the velocity record in X and Y axes. These were denoted as computer-identified axial dyskinesias. Around these computer-identified axial dyskinesias, there were large changes in X/Y/Z position, speed, acceleration, and angular velocity (Figure 3C–D).

As dyskinesias developed with two weeks of levodopa administration, average velocity increased, but not acceleration or angular velocity ($F_{(2,14)}$= 4.8, p<0.05; Figure 3E). Consistent with AIM scoring, there were more computer-identified axial dyskinesias on Day

13 vs. Day 1 of levodopa ($F_{(2,14)}$= 4.6, p<0.05; Figure 3F) and these increases were significantly correlated with AIM scores (R=0.73, p<0.01; Figure 3G). Our data indicate that computer-identified axial dyskinesias correlate with AIM scores, which have low temporal resolution (Breger et al., 2013; Sgroi et al., 2014). Indeed, around axial dyskinesias, automated tracking captured patterns of large displacements and faster movements. Automated tracking revealed that dyskinetic sessions are characterized by more overall movement and higher average velocity. Thus, such automated tracking techniques could be useful in capturing dyskinetic movements in mouse models of LIDs with high temporal resolution and linking these movements to striatal neuronal activity.

Striatal neurons and development of LIDs

Prior work demonstrates that striatal MSNs and FSIs encode aspects of movement (Berke et al., 2004; Berke, 2008; Hernandez et al., 2013; Jin et al., 2014; Barter et al., 2015a, 2015b). To examine striatal function during dyskinesias, we recorded striatal neuronal ensembles and tracked movement. In accordance with prior work, we used peak-to-trough duration and half-peak-width spike-waveforms to identify striatal MSNs and FSIs (Berke et al., 2004; Jin et al., 2014; Figure 4A). Gaussian mixture models were able to cluster striatal MSNs and striatal FSIs (Figure 4B). Across five 6-OHDA-lesion animals and four sham-lesion animals in three recording sessions (Saline, Day 1, and Day 13 of levodopa) we classified 240 neurons as MSNs and 146 as FSIs. Without levodopa administration dopamine-depleted animals had higher firing rates of MSNs (4.15 Hz ± 1.84) compared to shamlesioned animals (1.18 ± 0.56; $t_{(7)}$ = 3.6, p<0.01; Figure 4C). However, the firing rate of FSIs did not differ between dopamine depleted animals and sham-lesion animals (Figure 4C). For MSNs, a repeated measures ANOVA revealed main effects of lesion ($F_{(1,171)}$ = 5.60, p < 0.02) and levodopa administration ($F_{(1,171)}$ = 23.0, p < 10^{-5}) without interactions. The average firing rate of striatal MSNs was significantly higher on Day 13 (4.81 Hz ± 0.65) when compared to Day 1 (3.37 Hz ± 1.25) while FSIs on average were unchanged (Figure 4C).

We focused on Day 13 of levodopa sessions, as this time point had the most LIDs (Day 13; Figure 3F). In LID sessions after two weeks of levodopa injection (Day 13 of levodopa), we recorded 39 MSNs and 31 FSIs. Around axial dyskinesias, both striatal MSNs and FSIs had prominent modulations (Figure 5A–D). We found no clear evidence that MSNs and FSIs had differential patterns of activity around LIDs. These data indicate that both MSNs and FSIs could be strongly modulated around dyskinetic events.

Striatal field potentials and LIDs

Striatal LFPs reflect the integrated activity of striatal neurons. LFPs are prominently modulated by levodopa and could be a neurophysiological signature of LIDs that can be measured in humans (Brown et al., 2001; Brown, 2003; Brown and Williams, 2005). To investigate striatal LFPs in LID sessions, we recorded striatal LFPs and measured delta (1–4 Hz), theta (5–8 Hz), beta (12–24 Hz), and gamma band (25–95 Hz). Around computer-identified axial dyskinesias on Day 13, striatal LFPs had significant delta, theta, and beta modulations around axial dyskinesias (compared to random events; Figure 6A–B). Delta, beta, and gamma power significantly increased from Day 1 vs Day 13 of levodopa (delta: paired-$t_{(19)}$ = 3.4, p < 0.003; beta: paired-$t_{(19)}$ = 2.8, p < 0.01; gamma: paired-$t_{(19)}$ = 3.5, p <

0.003; data from 20 channels in 5 mice; Figure 6C–D). Additionally, we found that the 75–85 Hz power in dyskinetic animals was significantly higher (Day 13 vs Day 1; paired $t_{(19)} = 5.6$, $p < 10^{-5}$), similar to that previously reported in the motor cortex in dyskinetic rats (Halje et al., 2012). The LFPs in the sham lesion animals did not change from Day 1 to Day 13 of levodopa injections (Figure 6D). These data implicate delta, beta, and gamma bands in axial LIDs.

Next, we examined how spectral power in striatal LFPs was related to individual neuronal activity using spike-field coherence (Halliday et al., 1998). This technique allows us to investigate the evolution of coupling between individual neurons and striatal LFPs (Halliday et al., 1998; Narayanan et al., 2013; Parker et al., 2014). We normalized coherence values to the 95% confidence interval to compare raw spike-field coherence; thus a scaled coherence measure above 1 is significant at $p<0.05$ (Parker et al., 2015a). This measure revealed significant average delta spike-field coherence for FSIs but not for MSNs around axial LIDs (Figure 7A–B). Across all ensembles, we found that delta coherence in FSIs increased on Day 13 of levodopa administration compared to Day 1 (Figure 7A–D; $\chi^2=5.8$, $p<0.02$), whereas theta, beta, and gamma coherence did not. No changes were observed in MSNs on Day 1 vs Day 13 of levodopa, although levodopa administration did decrease delta spike-field coherence for MSNs (Saline vs Day 1, $\chi^2=4.7$, $p<0.03$; Figure 7C). Taken together, these data implicate delta-band striatal LFPs and delta spike-field coherence in dyskinesias and provide some insight into striatal network function in LIDs.

DISCUSSION

In the present study, we recorded from striatal neurons in unilaterally dopamine-depleted mice as they developed LIDs. We developed a novel automated tracking system to capture dyskinetic movements with high temporal resolution, allowing us to correlate dyskinesias with neuronal activity. Striatal MSNs increased activity as dyskinesias developed, but both striatal MSNs and FSIs were modulated around dyskinetic events. Furthermore, striatal LFPs increased delta and theta activity as dyskinesias developed, and striatal FSIs but not MSNs developed delta coupling during dyskinesias. To our knowledge, these are the first data to describe striatal network activity as dyskinesias develop, and suggest that dyskinesias change striatal network activity. This observation could help understand the disruption of striatal circuits during dyskinetic movements.

The dopamine precursor levodopa can influence the firing rate of MSNs (Centonze et al., 2003). Dopamine's effect on FSIs in unclear as it can increase excitability (Bracci et al., 2002) although this is not universally described with prolonged dopamine depletion (Mallet et al., 2006; Gittis et al., 2010). We do not observe consistent changes in FSI activity with dopamine depletion or repeated application of dopamine precursors. Dopamine depletion leads to complex changes in the circuitry of the striatum (Nisenbaum et al., 1986; Pang et al., 2001; Fino et al., 2007; Prosperetti et al., 2013; Corbit et al., 2016; Kondabolu et al., 2016). There have been few prior reports studying the activity of these striatal populations as LIDs develop (Picconi et al., 2003; Meissner et al., 2006; Liang et al., 2008; Belic et al., 2015). Though initial administration of levodopa significantly facilitates movement in humans and animal models, chronic exposure leads to severe side effects that can be

debilitating (Damiano et al., 2000; Péchevis et al., 2005). One important advance in our work is automated tracking with high temporal (<0 ms) and high spatial (< mm) resolution. Previous studies have largely relied on AIM scores, which can be laborious and temporally limited (Lundblad et al., 2004). Tracking techniques have been used to correlate movements with striatal neurophysiology (Barter et al., 2015a, 2015b), and here we extend this work to LIDs.

Previous work on LIDs provides evidence of increased expression of D1 dopamine receptors in the striatum in animals with LIDs, possibly implicating D1 MSNs in LIDs (Aubert et al., 2005; Darmopil et al., 2009; Hanrieder et al., 2011). Diverse changes in dopamine receptors and intracellular proteins with chronic levodopa administration could affect D1 and D2 MSN activity (Aubert et al., 2005 p.4; Darmopil et al., 2009; Bezard and Carta, 2015). Additionally, prior work on FSIs describe that under physiological conditions FSIs tend to preferentially target D1 MSNs (Gittis et al., 2011b), but following dopamine depletion FSIs showed higher connectivity to D2 MSNs (Gittis et al., 2011a). The change in inhibitory input to the different MSN populations may be a contributing factor in LIDs. Our study is limited in that we cannot differentiate between D1 and D2 MSNs, and we could not identify consistent synaptic relationships between MSNs and FSIs. Future studies in mice could try to unravel MSN-FSI interactions further and differentiate between D1 and D2 MSNs by recording simultaneously with optogenetics and pharmacology.

We found evidence of increased LFP delta, beta, and gamma rhythms after LIDs developed. Several prior studies have looked at the LFPs of dopamine-depleted animals during LIDs (Halje et al., 2012; Belic et al., 2015), and report the development of beta and gamma oscillations in the striatum. These beta oscillations can be increased with dyskinesias (Salvadè et al., 2016), and we find similar increases in beta and gamma rhythms here. However, we also report novel increases in delta power in LID sessions, and delta coupling with FSIs.

These data could provide insight into the mechanism of striatal network dysfunction during LIDs. FSIs express dopamine receptors, exert a powerful influence over MSNs, and, thus, modulate the firing of these neurons (Koós and Tepper, 1999; Bracci et al., 2002; Planert et al., 2010; Berke, 2011). FSIs have also been reported to have less-specific task modulations (Berke, 2008). With levodopa administration, FSIs might increase their firing and to suppress MSN activity. However, after LIDs develop, these FSIs are coupled to delta/beta rhythms, and, thus, might be unable to regulate MSN activity, leading to LIDs.

Our study is the first report to our knowledge that combines automated tracking in rodent models of LIDs with striatal neuronal ensemble recording. Our results are biased towards axial dyskinesias as the tracking device was placed on the animals' midline. Future advances in 3-dimensional tracking might enable high-fidelity tracking of these movements, and extend this work to limb dyskinesias and orofacial dyskinesias. Capturing these dyskinesias in freely-moving mice would require significant advances in tracking technology, but might afford a higher-resolution picture of striatal neuronal activity. However, because axial dyskinesias are a large component of LIDs, our results are representative of striatal changes with the development of LIDs (Winkler et al., 2002).

One further limitation includes our LID protocol. Electrode implants are expensive and labor intensive; thus, we used a lower dose of 6-OHDA and a higher levodopa dose to minimize mortality while maximize LIDs (Pan and Walters, 1988; Duty and Jenner, 2011; Thiele et al., 2012). While this protocol produced reliable LIDs in our hands, some aspects of our results might be difficult to compare to prior work. Additionally, we allowed animals to recover for one week before starting levodopa treatment, while other studies allow animals to recover for three weeks. Levodopa therapy is typically used early in PD treatment while dopaminergic neuronal death is still occurring and within 4–6 years of treatment about 40% of patients develop LIDs (Ahlskog and Muenter, 2001; Kumar et al., 2005); thus our data might still have clinical relevance, although our interpretation is complicated by ongoing dopaminergic cell loss. Despite these limitations, our data clearly indicate that we can use automated methods to track LIDs and correlate these events with striatal neuronal activity, and that striatal MSNs and LFPs change as LIDs develop.

Conclusions

We have developed an automated tracking system to capture striatal neuronal activity around axial LIDs. We found that both striatal MSNs and FSIs are strongly modulated around dyskinetic events. Only FSIs were coupled with increased striatal delta power as LIDs developed. These data provide insight into how striatal networks change as LIDs develop as well as new tools to analyze LIDs in detail.

Acknowledgments

This study was funded by a Ruth L. Kirschstein National Research Service Award (1 F31 NS092190-01) and Dr. Narayanan's R01 (NS089470). These funding sources did not partake in study design, data collection and analysis, or the drafting and submission of this manuscript.

REFERENCES

Ahlskog JE, Muenter MD. Frequency of levodopa-related dyskinesias and motor fluctuations as estimated from the cumulative literature. Mov Disord Off J Mov Disord Soc. 2001; 16:448–458.

Alberico SL, Cassell MD, Narayanan NS. The Vulnerable Ventral Tegmental Area in Parkinson's Disease. Basal Ganglia. 2015; 5:51–55. [PubMed: 26251824]

Aubert I, Guigoni C, Håkansson K, Li Q, Dovero S, Barthe N, Bioulac BH, Gross CE, Fisone G, Bloch B, Bezard E. Increased D1 dopamine receptor signaling in levodopa-induced dyskinesia. Ann Neurol. 2005; 57:17–26. [PubMed: 15514976]

Barter JW, Li S, Lu D, Bartholomew RA, Rossi MA, Shoemaker CT, Salas-Meza D, Gaidis E, Yin HH. Beyond reward prediction errors: the role of dopamine in movement kinematics. Front Integr Neurosci. 2015a; 9 [Accessed January 26, 2016] Available at: http://www.ncbi.nlm.nih.gov/pmc/articles/PMC4444742/.

Barter JW, Li S, Sukharnikova T, Rossi MA, Bartholomew RA, Yin HH. Basal Ganglia Outputs Map Instantaneous Position Coordinates during Behavior. J Neurosci. 2015b; 35:2703–2716. [PubMed: 25673860]

Belic J, Halje P, Richter U, Petersson P, Hellgren Kotaleski J. Untangling cortico-striatal connectivity and cross-frequency coupling in L-DOPA-induced dyskinesia. 2015 [Accessed January 21, 2016] Available at: http://biorxiv.org/lookup/doi/10.1101/028027.

Berke JD. Uncoordinated Firing Rate Changes of Striatal Fast-Spiking Interneurons during Behavioral Task Performance. J Neurosci. 2008; 28:10075–10080. [PubMed: 18829965]

Berke JD. Functional properties of striatal fast-spiking interneurons. Front Syst Neurosci. 2011; 5:45. [PubMed: 21743805]

Berke JD, Okatan M, Skurski J, Eichenbaum HB. Oscillatory Entrainment of Striatal Neurons in Freely Moving Rats. Neuron. 2004; 43:883–896. [PubMed: 15363398]

Bezard E, Carta M. Could the serotonin theory give rise to a treatment for levodopa-induced dyskinesia in Parkinson's disease? Brain J Neurol. 2015; 138:829–830.

Bido S, Marti M, Morari M. Amantadine attenuates levodopa-induced dyskinesia in mice and rats preventing the accompanying rise in nigral GABA levels. J Neurochem. 2011; 118:1043–1055. [PubMed: 21740438]

Bracci E, Centonze D, Bernardi G, Calabresi P. Dopamine excites fast-spiking interneurons in the striatum. J Neurophysiol. 2002; 87:2190–2194. [PubMed: 11929936]

Breger LS, Dunnett SB, Lane EL. Comparison of rating scales used to evaluate l-DOPA-induced dyskinesia in the 6-OHDA lesioned rat. Neurobiol Dis. 2013; 50:142–150. [PubMed: 23072976]

Brown P. Oscillatory nature of human basal ganglia activity: relationship to the pathophysiology of Parkinson's disease. Mov Disord Off J Mov Disord Soc. 2003; 18:357–363.

Brown P, Oliviero A, Mazzone P, Insola A, Tonali P, Lazzaro VD. Dopamine Dependency of Oscillations between Subthalamic Nucleus and Pallidum in Parkinson's Disease. J Neurosci. 2001; 21:1033–1038. [PubMed: 11157088]

Brown P, Williams D. Basal ganglia local field potential activity: Character and functional significance in the human. Clin Neurophysiol. 2005; 116:2510–2519. [PubMed: 16029963]

Bunney BS, Aghajanian GK, Roth RH. Comparison of effects of L-dopa, amphetamine and apomorphine on firing rate of rat dopaminergic neurones. Nature New Biol. 1973; 245:123–125. [PubMed: 4518113]

Cenci MA, Lundblad M. Ratings of L-DOPA-induced dyskinesia in the unilateral 6-OHDA lesion model of Parkinson's disease in rats and mice. Curr Protoc Neurosci Editor Board Jacqueline N Crawley Al. 2007; Chapter 9(Unit 9):25.

Centonze D, Grande C, Usiello A, Gubellini P, Erbs E, Martin AB, Pisani A, Tognazzi N, Bernardi G, Moratalla R, Borrelli E, Calabresi P. Receptor subtypes involved in the presynaptic and postsynaptic actions of dopamine on striatal interneurons. J Neurosci Off J Soc Neurosci. 2003; 23:6245–6254.

Chang JW, Wachtel SR, Young D, Kang UJ. Biochemical and anatomical characterization of forepaw adjusting steps in rat models of Parkinson's disease: studies on medial forebrain bundle and striatal lesions. Neuroscience. 1999; 88:617–628. [PubMed: 10197780]

Chotibut T, Davis RW, Arnold JC, Frenchek Z, Gurwara S, Bondada V, Geddes JW, Salvatore MF. Ceftriaxone increases glutamate uptake and reduces striatal tyrosine hydroxylase loss in 6-OHDA Parkinson's model. Mol Neurobiol. 2013; 49:1282–1292. [PubMed: 24297323]

Corbit VL, Whalen TC, Zitelli KT, Crilly SY, Rubin JE, Gittis AH. Pallidostriatal Projections Promote beta Oscillations in a Dopamine-Depleted Biophysical Network Model. J Neurosci Off J Soc Neurosci. 2016; 36:5556–5571.

Cui G, Jun SB, Jin X, Pham MD, Vogel SS, Lovinger DM, Costa RM. Concurrent activation of striatal direct and indirect pathways during action initiation. Nature. 2013; 494:238–242. [PubMed: 23354054]

Damiano AM, McGrath MM, Willian MK, Snyder CF, LeWitt PA, Reyes PF, Richter RR, Means ED. Evaluation of a measurement strategy for Parkinson's disease: assessing patient health-related quality of life. Qual Life Res Int J Qual Life Asp Treat Care Rehabil. 2000; 9:87–100.

Darmopil S, Martín AB, De Diego IR, Ares S, Moratalla R. Genetic Inactivation of Dopamine D1 but Not D2 Receptors Inhibits L-DOPA–Induced Dyskinesia and Histone Activation. Biol Psychiatry. 2009; 66:603–613. [PubMed: 19520364]

Delorme A, Makeig S. EEGLAB: an open source toolbox for analysis of single-trial EEG dynamics including independent component analysis. J Neurosci Methods. 2004; 134:9–21. [PubMed: 15102499]

Duty S, Jenner P. Animal models of Parkinson's disease: a source of novel treatments and clues to the cause of the disease. Br J Pharmacol. 2011; 164:1357–1391. [PubMed: 21486284]

Emmons EB, Ruggiero RN, Kelley RM, Parker KL, Narayanan NS. Corticostriatal Field Potentials Are Modulated at Delta and Theta Frequencies during Interval-Timing Task in Rodents. Front

Psychol. 2016; 7 [Accessed April 25, 2016] Available at: http://www.ncbi.nlm.nih.gov/pmc/articles/PMC4820903/.

Fahn S, Oakes D, Shoulson I, Kieburtz K, Rudolph A, Lang A, Olanow CW, Tanner C, Marek K. Levodopa and the progression of Parkinson's disease. N Engl J Med. 2004; 351:2498–2508. [PubMed: 15590952]

Fino E, Glowinski J, Venance L. Effects of acute dopamine depletion on the electrophysiological properties of striatal neurons. Neurosci Res. 2007; 58:305–316. [PubMed: 17499375]

Gerfen CR. Molecular effects of dopamine on striatal-projection pathways. Trends Neurosci. 2000; 23:S64–S70. [PubMed: 11052222]

Gittis AH, Hang GB, LaDow ES, Shoenfeld LR, Atallah BV, Finkbeiner S, Kreitzer AC. Rapid target-specific remodeling of fast-spiking inhibitory circuits after loss of dopamine. Neuron. 2011a; 71:858–868. [PubMed: 21903079]

Gittis AH, Leventhal DK, Fensterheim BA, Pettibone JR, Berke JD, Kreitzer AC. Selective inhibition of striatal fast-spiking interneurons causes dyskinesias. J Neurosci Off J Soc Neurosci. 2011b; 31:15727–15731.

Gittis AH, Nelson AB, Thwin MT, Palop JJ, Kreitzer AC. Distinct roles of GABAergic interneurons in the regulation of striatal output pathways. J Neurosci Off J Soc Neurosci. 2010; 30:2223–2234.

Halje P, Tamtè M, Richter U, Mohammed M, Cenci MA, Petersson P. Levodopa-Induced Dyskinesia Is Strongly Associated with Resonant Cortical Oscillations. J Neurosci. 2012; 32:16541–16551. [PubMed: 23175810]

Halliday DM, Conway BA, Farmer SF, Rosenberg JR. Using electroencephalography to study functional coupling between cortical activity and electromyograms during voluntary contractions in humans. Neurosci Lett. 1998; 241:5–8. [PubMed: 9502202]

Halliday DM, Rosenberg JR, Amjad AM, Breeze P, Conway BA, Farmer SF. A framework for the analysis of mixed time series/point process data—Theory and application to the study of physiological tremor, single motor unit discharges and electromyograms. Prog Biophys Mol Biol. 1995; 64:237–278. [PubMed: 8987386]

Hanrieder J, Ljungdahl A, Fälth M, Mammo SE, Bergquist J, Andersson M. L-DOPA-induced dyskinesia is associated with regional increase of striatal dynorphin peptides as elucidated by imaging mass spectrometry. Mol Cell Proteomics MCP. 2011; 10 M111.009308.

Healy-Stoffel M, Ahmad SO, Stanford JA, Levant B. A novel use of combined tyrosine hydroxylase and silver nucleolar staining to determine the effects of a unilateral intrastriatal 6-hydroxydopamine lesion in the substantia nigra: A stereological study. J Neurosci Methods. 2012; 210:187–194. [PubMed: 22850559]

Hernandez LF, Kubota Y, Hu D, Howe MW, Lemaire N, Graybiel AM. Selective Effects of Dopamine Depletion and L-DOPA Therapy on Learning-Related Firing Dynamics of Striatal Neurons. J Neurosci. 2013; 33:4782–4795. [PubMed: 23486949]

Jenkinson N, Brown P. New insights into the relationship between dopamine, beta oscillations and motor function. Trends Neurosci. 2011; 34:611–618. [PubMed: 22018805]

Jin X, Tecuapetla F, Costa RM. Basal ganglia subcircuits distinctively encode the parsing and concatenation of action sequences. Nat Neurosci. 2014; 17:423–430. [PubMed: 24464039]

Kondabolu K, Roberts EA, Bucklin M, McCarthy MM, Kopell N, Han X. Striatal cholinergic interneurons generate beta and gamma oscillations in the corticostriatal circuit and produce motor deficits. Proc Natl Acad Sci U S A. 2016; 113:E3159–E3168. [PubMed: 27185924]

Koós T, Tepper JM. Inhibitory control of neostriatal projection neurons by GABAergic interneurons. Nat Neurosci. 1999; 2:467–472. [PubMed: 10321252]

Koos T, Tepper JM, Wilson CJ. Comparison of IPSCs Evoked by Spiny and Fast-Spiking Neurons in the Neostriatum. J Neurosci. 2004; 24:7916–7922. [PubMed: 15356204]

Kreitzer AC. Physiology and Pharmacology of Striatal Neurons. Annu Rev Neurosci. 2009; 32:127–147. [PubMed: 19400717]

Kumar N, Van Gerpen JA, Bower JH, Ahlskog JE. Levodopa-dyskinesia incidence by age of Parkinson's disease onset. Mov Disord. 2005; 20:342–344. [PubMed: 15580606]

Liang L, DeLong MR, Papa SM. Inversion of Dopamine Responses in Striatal Medium Spiny Neurons and Involuntary Movements. J Neurosci. 2008; 28:7537–7547. [PubMed: 18650331]

Lundblad M, Andersson M, Winkler C, Kirik D, Wierup N, Cenci MA. Pharmacological validation of behavioural measures of akinesia and dyskinesia in a rat model of Parkinson's disease. Eur J Neurosci. 2002; 15:120–132. [PubMed: 11860512]

Lundblad M, Picconi B, Lindgren H, Cenci MA. A model of l-DOPA-induced dyskinesia in 6-hydroxydopamine lesioned mice: relation to motor and cellular parameters of nigrostriatal function. Neurobiol Dis. 2004; 16:110–123. [PubMed: 15207268]

Lundblad M, Usiello A, Carta M, Håkansson K, Fisone G, Cenci MA. Pharmacological validation of a mouse model of l-DOPA-induced dyskinesia. Exp Neurol. 2005; 194:66–75. [PubMed: 15899244]

Mallet N, Ballion B, Moine CL, Gonon F. Cortical Inputs and GABA Interneurons Imbalance Projection Neurons in the Striatum of Parkinsonian Rats. J Neurosci. 2006; 26:3875–3884. [PubMed: 16597742]

Meissner W, Ravenscroft P, Reese R, Harnack D, Morgenstern R, Kupsch A, Klitgaard H, Bioulac B, Gross CE, Bezard E, Boraud T. Increased slow oscillatory activity in substantia nigra pars reticulata triggers abnormal involuntary movements in the 6-OHDA-lesioned rat in the presence of excessive extracelullar striatal dopamine. Neurobiol Dis. 2006; 22:586–598. [PubMed: 16531050]

Narayanan NS, Cavanagh JF, Frank MJ, Laubach M. Common neural correlates of adaptive control in the anterior cingulate cortex of rats and humansCommon neural co. 2013

Nisenbaum ES, Stricker EM, Zigmond MJ, Berger TW. Long-term effects of dopamine-depleting brain lesions on spontaneous activity of type II striatal neurons: Relation to behavioral recovery. Brain Res. 1986; 398:221–230. [PubMed: 3099976]

Pang Z, Ling GY, Gajendiran M, Xu ZC. Enhanced excitatory synaptic transmission in spiny neurons of rat striatum after unilateral dopamine denervation. Neurosci Lett. 2001; 308:201–205. [PubMed: 11479023]

Pan HS, Walters JR. Unilateral lesion of the nigrostriatal pathway decreases the firing rate and alters the firing pattern of globus pallidus neurons in the rat. Synap N Y N. 1988; 2:650–656.

Paquette MA, Foley K, Brudney EG, Meshul CK, Johnson SW, Berger SP. The sigma-1 antagonist BMY-14802 inhibits L-DOPA-induced abnormal involuntary movements by a WAY-100635-sensitive mechanism. Psychopharmacology (Berl). 2009; 204:743–754. [PubMed: 19283364]

Parker KL, Chen K-H, Kingyon JR, Cavanagh JF, Narayanan NS. D1-Dependent 4 Hz Oscillations and Ramping Activity in Rodent Medial Frontal Cortex during Interval Timing. J Neurosci. 2014; 34:16774–16783. [PubMed: 25505330]

Parker KL, Chen K-H, Kingyon JR, Cavanagh JF, Naryanan NS. Medial frontal ~4 Hz activity in humans and rodents is attenuated in PD patients and in rodents with cortical dopamine depletion. J Neurophysiol:jn. 2015a 00412.2015.

Parker KL, Ruggiero RN, Narayanan NS. Infusion of D1 Dopamine Receptor Agonist into Medial Frontal Cortex Disrupts Neural Correlates of Interval Timing. Front Behav Neurosci. 2015b; 9:294. [PubMed: 26617499]

Pavón N, Martín AB, Mendialdua A, Moratalla R. ERK Phosphorylation and FosB Expression Are Associated with L-DOPA-Induced Dyskinesia in Hemiparkinsonian Mice. Biol Psychiatry. 2006; 59:64–74. [PubMed: 16139809]

Péchevis M, Clarke CE, Vieregge P, Khoshnood B, Deschaseaux-Voinet C, Berdeaux G, Ziegler M. Trial Study Group. Effects of dyskinesias in Parkinson's disease on quality of life and health-related costs: a prospective European study. Eur J Neurol. 2005; 12:956–963. [PubMed: 16324089]

Picconi B, Centonze D, Håkansson K, Bernardi G, Greengard P, Fisone G, Cenci MA, Calabresi P. Loss of bidirectional striatal synaptic plasticity in L-DOPA–induced dyskinesia. Nat Neurosci. 2003; 6:501–506. [PubMed: 12665799]

Planert H, Szydlowski SN, Hjorth JJJ, Grillner S, Silberberg G. Dynamics of Synaptic Transmission between Fast-Spiking Interneurons and Striatal Projection Neurons of the Direct and Indirect Pathways. J Neurosci. 2010; 30:3499–3507. [PubMed: 20203210]

Prosperetti C, Di Giovanni G, Stefani A, Moller JC, Galati S. Acute nigro-striatal blockade alters cortico-striatal encoding: an in vivo electrophysiological study. Exp Neurol. 2013; 247:730–736. [PubMed: 23537952]

Rosenberg JR, Amjad AM, Breeze P, Brillinger DR, Halliday DM. The Fourier approach to the identification of functional coupling between neuronal spike trains. Prog Biophys Mol Biol. 1989; 53:1–31. [PubMed: 2682781]

Salvadè A, D'Angelo V, Di Giovanni G, Tinkhauser G, Sancesario G, Städler C, Möller JC, Stefani A, Kaelin-Lang A, Galati S. Distinct roles of cortical and pallidal β and γ frequencies in hemiparkinsonian and dyskinetic rats. Exp Neurol. 2016; 275(Pt 1):199–208. [PubMed: 26571194]

Santini E, Valjent E, Usiello A, Carta M, Borgkvist A, Girault J-A, Hervé D, Greengard P, Fisone G. Critical involvement of cAMP/DARPP-32 and extracellular signal-regulated protein kinase signaling in L-DOPA-induced dyskinesia. J Neurosci Off J Soc Neurosci. 2007; 27:6995–7005.

Sgroi S, Kaelin-Lang A, Capper-Loup C. Spontaneous locomotor activity and L-DOPA-induced dyskinesia are not linked in 6-OHDA parkinsonian rats. Front Behav Neurosci. 2014; 8:331. [PubMed: 25324746]

Smith, GA., Heuer, A., Dunnett, SB., Lane, EL. [Accessed October 2, 2011] Unilateral nigrostriatal 6-hydroxydopamine lesions in mice II: Predicting l-DOPA-induced dyskinesia. Behav Brain Res. 2011. Available at: http://www.ncbi.nlm.nih.gov/pubmed/21946310

Surmeier DJ, Ding J, Day M, Wang Z, Shen W. D1 and D2 dopamine-receptor modulation of striatal glutamatergic signaling in striatal medium spiny neurons. Trends Neurosci. 2007; 30:228–235. [PubMed: 17408758]

Thiele, SL., Warre, R., Nash, JE. [Accessed September 13, 2016] Development of a Unilaterally-lesioned 6-OHDA Mouse Model of Parkinson's Disease. J Vis Exp JoVE. 2012. Available at: http://www.ncbi.nlm.nih.gov/pmc/articles/PMC3376941/

Williams D, Tijssen M, Van Bruggen G, Bosch A, Insola A, Di Lazzaro V, Mazzone P, Oliviero A, Quartarone A, Speelman H, Brown P. Dopamine-dependent changes in the functional connectivity between basal ganglia and cerebral cortex in humans. Brain J Neurol. 2002; 125:1558–1569.

Winkler C, Kirik D, Björklund A, Cenci MA. l-DOPA-Induced Dyskinesia in the Intrastriatal 6-Hydroxydopamine Model of Parkinson's Disease: Relation to Motor and Cellular Parameters of Nigrostriatal Function. Neurobiol Dis. 2002; 10:165–186. [PubMed: 12127155]

ABBREVIATIONS

PD	Parkinson's disease
LIDs	levodopa-induced dyskinesias
AIM	abnormal involuntary movement
MSN	medium spiny neuron
FSI	fast spiking interneuron
LFP	local field potential
MFB	medial forebrain bundle

HIGHLIGHTS

- We developed an automated system to track levodopa-induced dyskinesias in mice.
- Striatal medium spiny neurons and fast spiking interneurons were modulated around dyskinesias.
- Delta power and delta-neuronal coupling increased as dyskinesias developed.

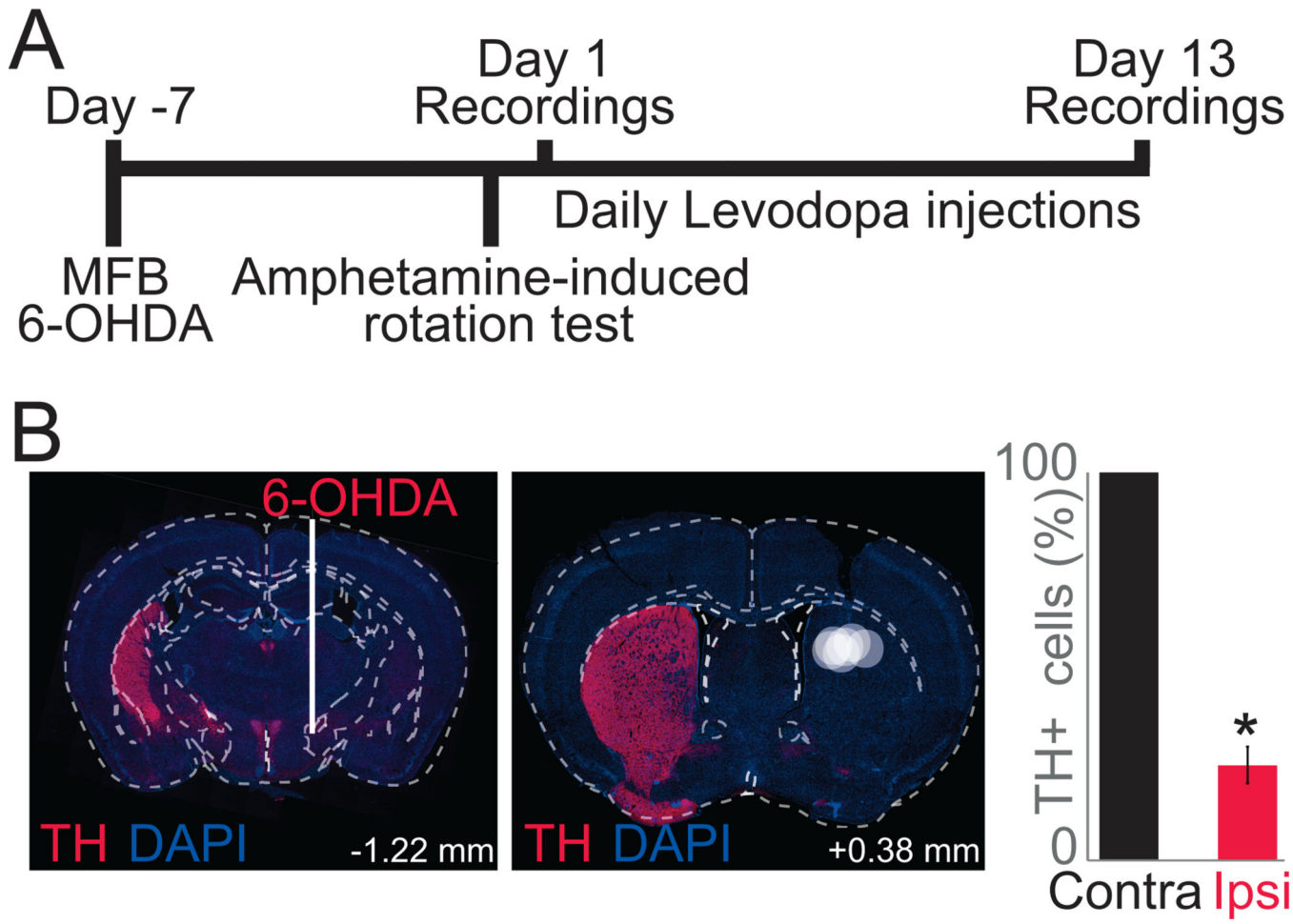

Figure 1. Experimental timeline: mouse model of levodopa-induced dyskinesias

A) To model LIDs, we depleted dopamine unilaterally with a MFB 6-OHDA lesion and injected levodopa (20 mg/kg) for two weeks. We recorded striatal neuronal ensemble activity on Day 1 and 13 of levodopa administration. B) Location of MFB 6-OHDA lesion (left) via immunohistochemistry resulting in large loss of striatal dopamine in the dorsal striatum, where electrodes were implanted (right; TH in red; DAPI in blue). Each white circle represents electrode placement of one animal. Bar graph shows quantification of TH in the substantia nigra pars compacta. On average, animals had 71±5% less TH positive cells on the lesioned side (red) when compared to the contralateral side (black). Data from 5 lesioned mice. (*) $p<0.05$.

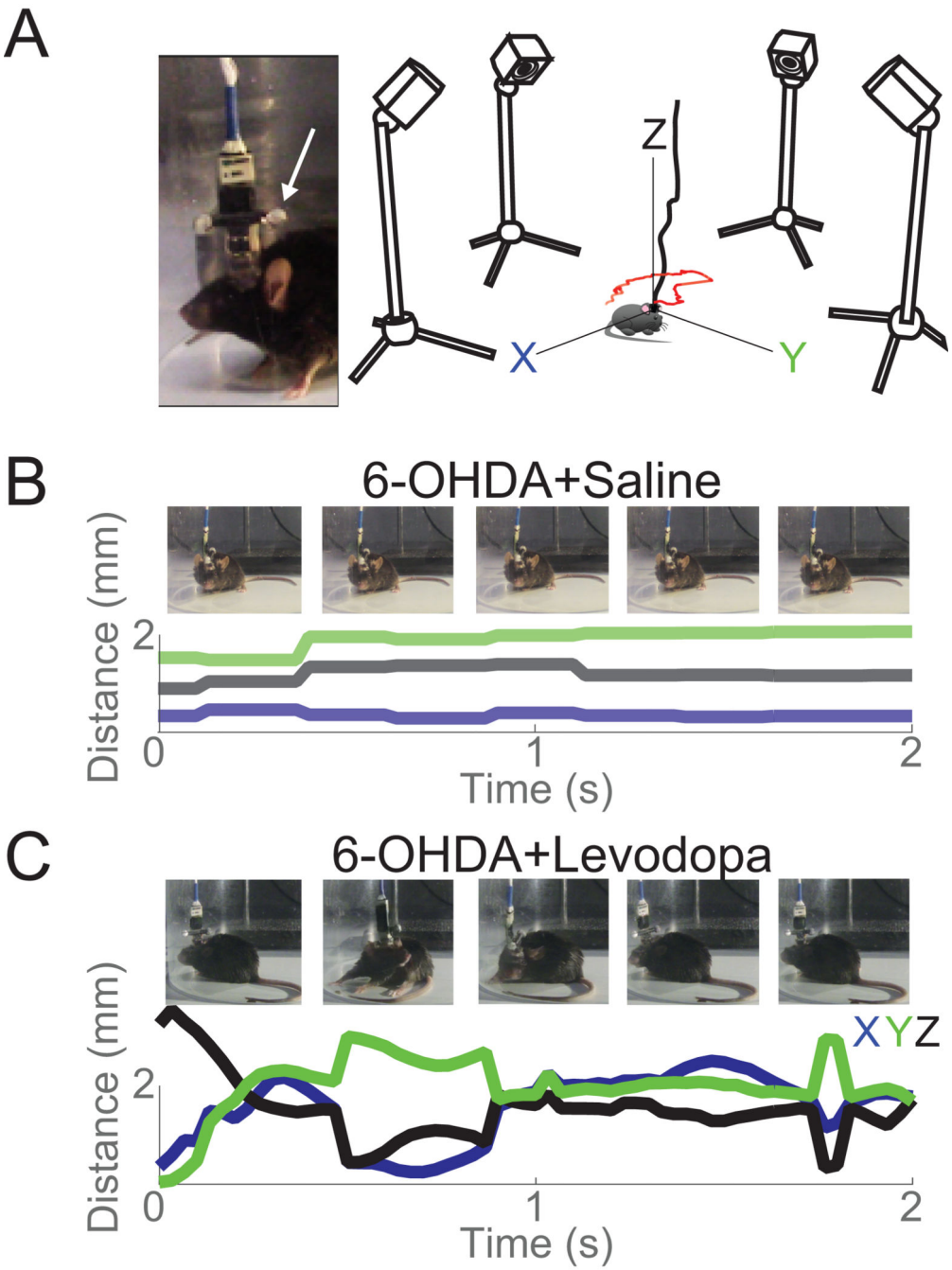

Figure 2. Tracking set-up

A) Inset: Picture of two infrared reflective spheres (white arrow) and recording electrode. Right: Diagram of 4 infrared cameras calibrated to track movements at 120 frames/s. B) Tracking examples (2 s) in a dopamine-depleted animal (6-OHDA) in the X (blue), Y (green), and Z (black) axes with corresponding still images. C) The same animal as in (B) with initial levodopa administration in the X (blue), Y (green), and Z (black) axes with corresponding still images.

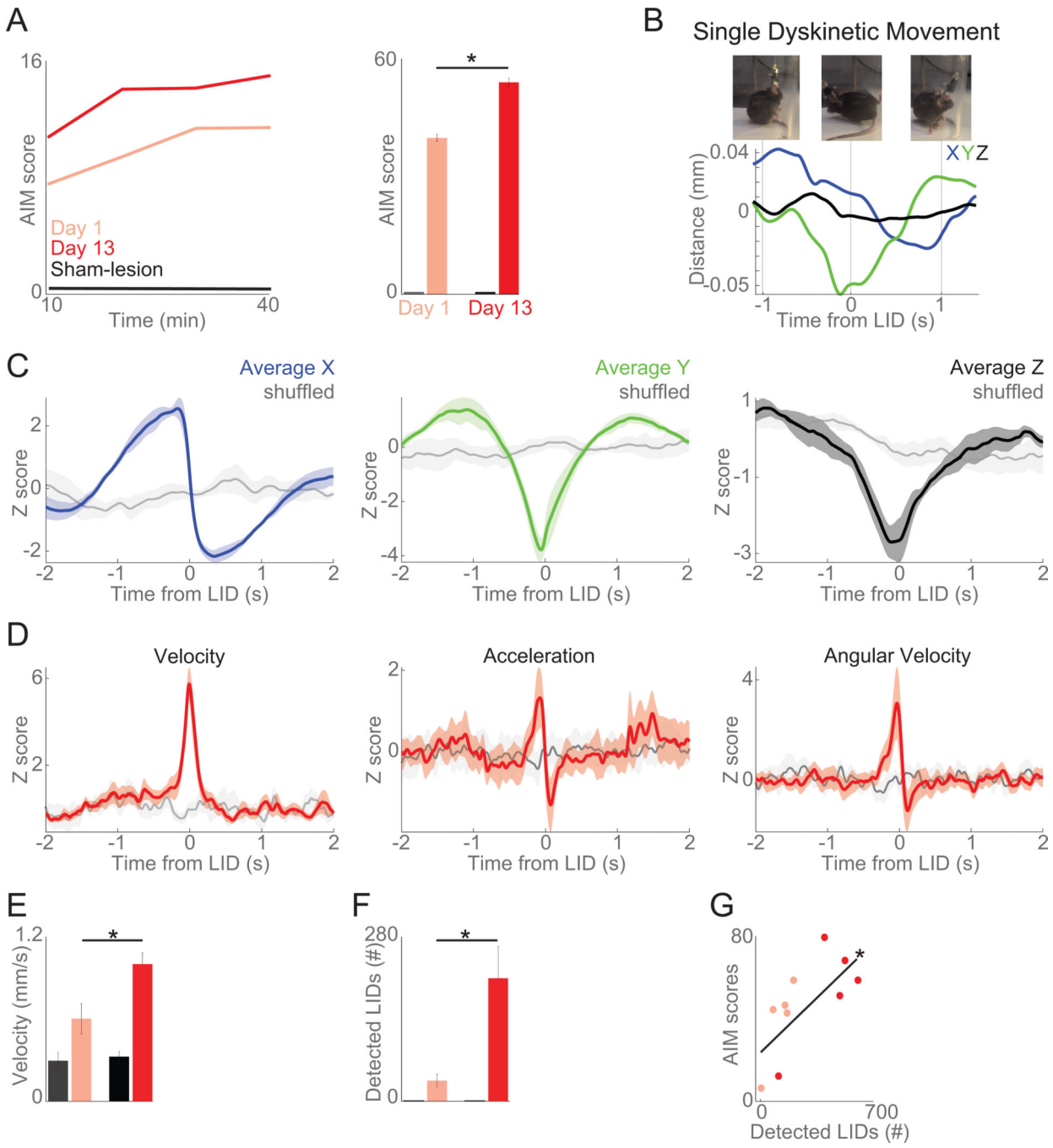

Figure 3. Automated tracking of axial LIDs

A) With levodopa administration for two weeks, LIDs increased over time by AIM scoring in 6-OHDA-lesioned animals (5 animals) but not sham-lesioned animals (4 mice). B) Example traces from one mouse 1 s before and after a single hand-coded axial LID on all three axes (X: blue, Y: green, Z: black). C) Average displacement observed around the computer-identified axial LIDs in all three axes (X: blue, Y: green, Z: black) compared to shuffled events (noise, in gray; based on randomly selected timestamps). D) Around computer-identified events, there were large changes in velocity, acceleration, and angular

velocity when compared to shuffled data (gray). E) Average velocity increased as LIDs developed, while acceleration and angular velocity did not. F) Computer-identified dyskinetic events increased as LIDs developed. G) Computer-detected LIDs and AIM scores were significantly correlated. These data indicate that automated motion tracking can capture axial dyskinesias. Data from five 6-OHDA-lesioned and four sham-lesioned mice. Error bars are mean ± SEM. (*) $p<0.05$.

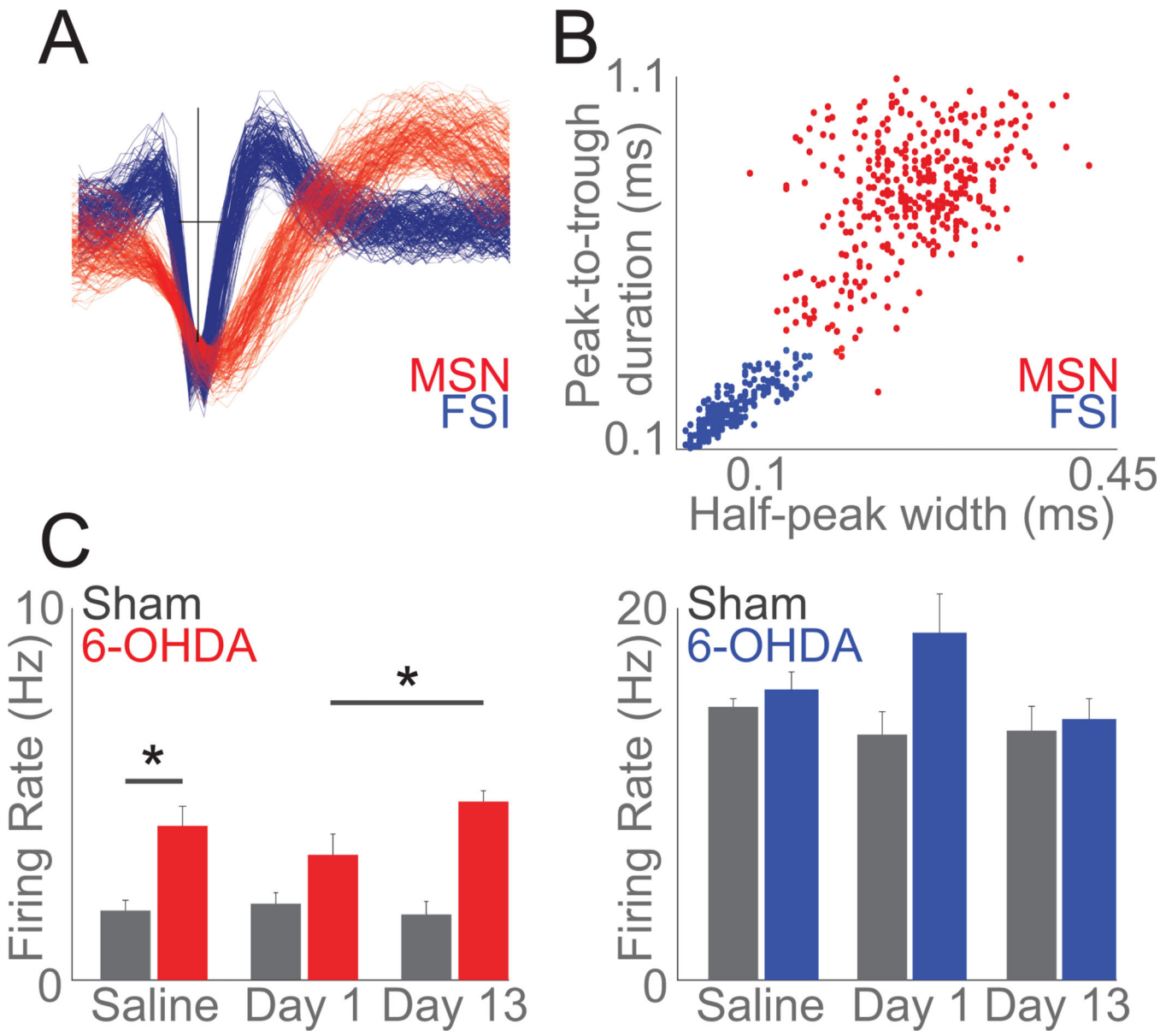

Figure 4. Striatal MSNs increase firing rate as LIDs develop

A) Example waveforms of one MSN (red) and one FSI (blue) recorded from a single electrode. B) Clustering across peak-to-trough duration and half-peak-width identified 240 MSNs (red) and 146 FSIs (blue). C) Mean firing rate of MSNs increased following 6-OHDA lesion (Saline: sham-lesion (grey) vs 6-OHDA-lesioned in (red)) and as LIDs developed (Day 1 vs Day 13) while FSIs did not change as LIDs developed; data from 240 MSNs and 146 FSIs in 9 mice over 3 days. Error bars are mean ± SEM; (*) $p<0.05$.

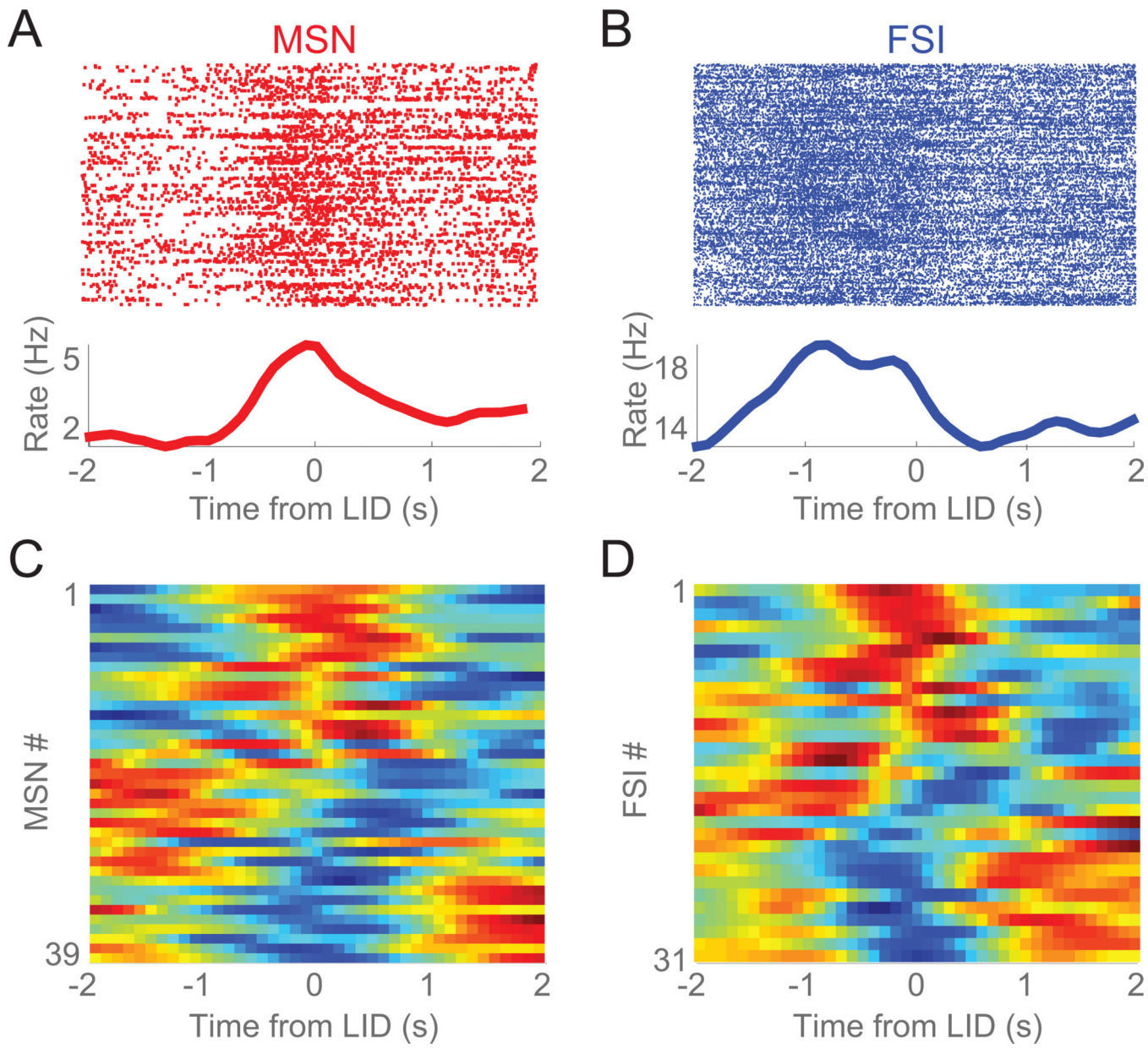

Figure 5. Striatal neurons are modulated around levodopa-induced dyskinesias

A) Example of an MSN and B) an FSI showing prominent firing rate modulation around computer-identified axial dyskinesias (0 s, Time from LID). Top portions are raster plots where each line represents a time-coded LID and each dot represents an action potential of the neurons. Bottom portions are the average firing rate for that neuron for all time-coded LIDs. C) Firing rate changes for all MSNs and D) all FSIs around axial dyskinesias on Day 13.

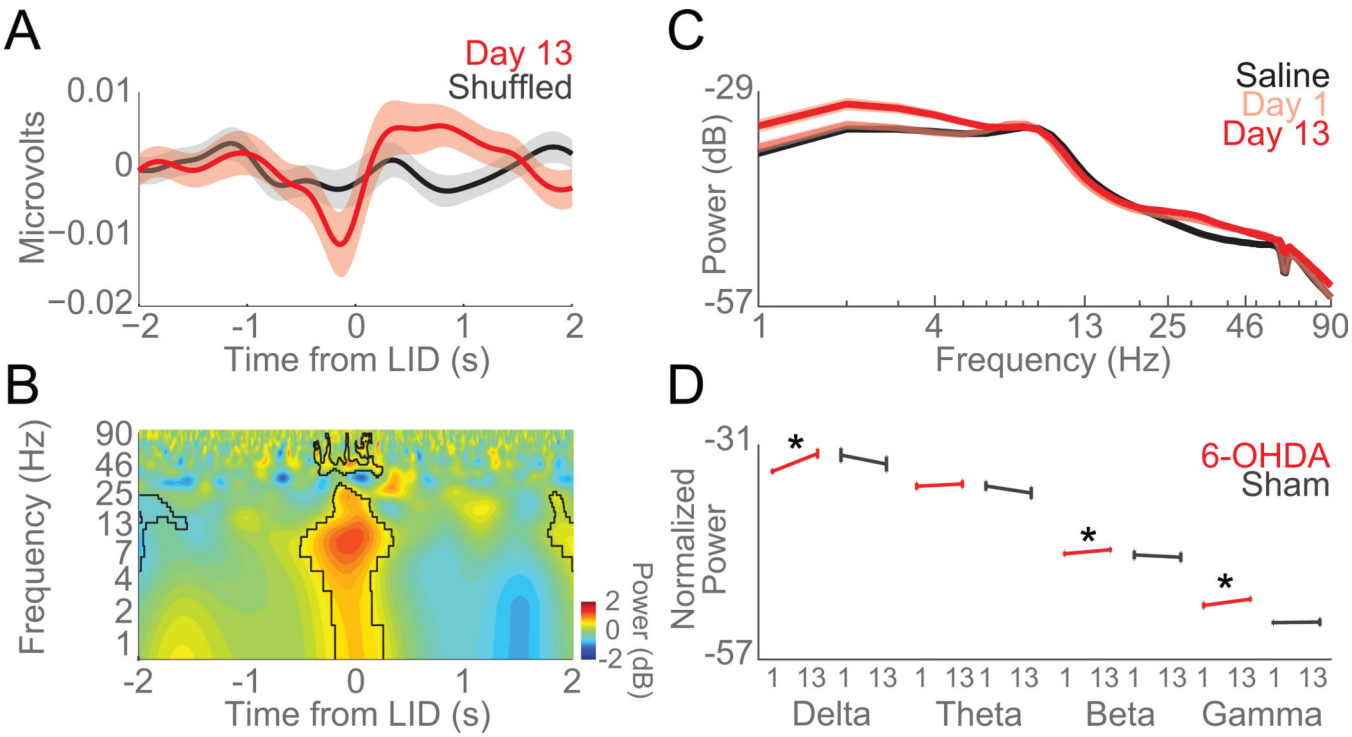

Figure 6. Delta power in striatal local field potentials increases as LIDs develop

A) Voltage modulation of LFPs around axial dyskinesias (0 s, Time from LID). B) Time-frequency plot of LFPs around axial dyskinesias. Spectral power of LFP activity revealed significant modulations in delta, theta, and beta bands around axial dyskinesias vs. shuffled events (outlined in black). C) Spectral power of striatal LFPs on Saline (black), Day 1 (pink), and Day 13 (red) of levodopa administration. D) Error bar of average normalized power (dB) of 6-OHDA-lesioned mice (red) and sham-lesioned mice (grey) in each frequency band across days (Day 1 and Day 13). Delta, beta, and gamma power significantly increased as LIDs developed in 6-OHDA-lesioned mice (red). No changes were seen in mice with sham lesions (grey). Data from five 6-OHDA-lesioned and four sham-lesioned mice. Error bars are mean ± SEM. (*) $p<0.05$.

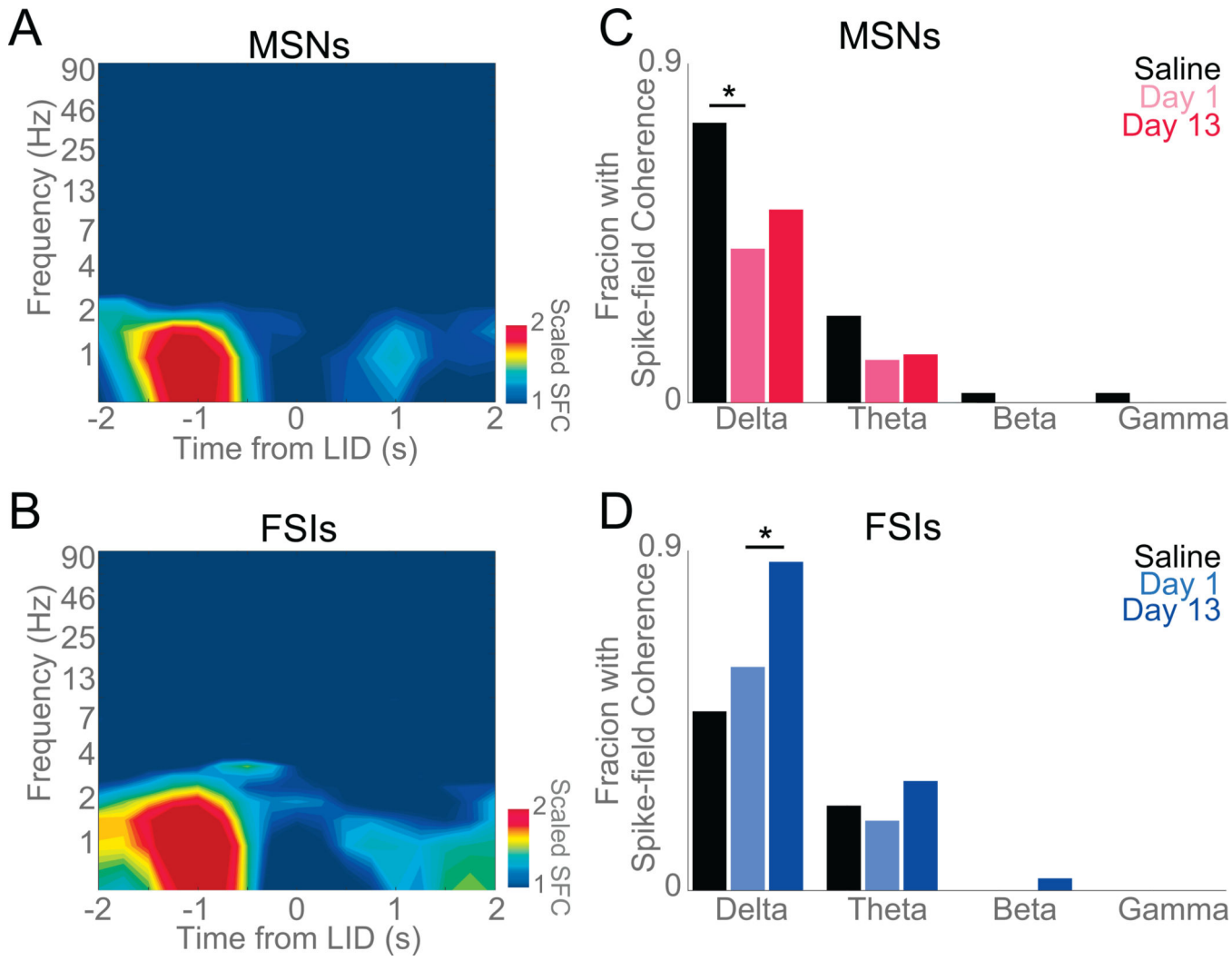

Figure 7. Striatal FSI delta spike-field coherence increases as LIDs develop

Normalized spike-field coherence around axial dyskinesias for A) MSNs and B) FSIs. All spike-field coherence was normalized to 95% significance; thus yellow and red indicate significant spike-field coherence. Data from 39 MSNs and 31 FSIs in five 6-OHDA-lesioned mice on Day 13 of levodopa. C) Initial administration of levodopa (Day 1) significantly reduced delta spike field-coherence in MSNs when compared to Saline but no change was detected as dyskinesias developed. D) FSIs significantly increased delta coherence as dyskinesias developed. Data from 5 mice. (*) $p<0.05$